CHANGES IN THE ATMOSPHERIC STRUCTURE OF LBV'S DURING ERUPTIONS

Claus Leitherer, David C. Abbott, and Werner Schmutz
Joint Institute for Laboratory Astrophysics
University of Colorado and National Bureau of Standards
Boulder, CO 80309-0440

I. INTRODUCTION

Some LBV's undergo brightness variations in the visual of about 1-2 magnitudes on time-scales of decades. These outbursts occur at approximately constant bolometric luminosity with the stellar radius and the temperature changing correspondingly. This subgroup of the LBV's is generally called Hubble-Sandage variables or S Doradus stars and will be the focus of this talk. We present self-consistent radiation-hydrodynamic calculations to model the observations from minimum to maximum states.

II. THE ATMOSPHERIC MODELS

Previous analyses of LBV's were based on models which made use of hydrostatic, plane-parallel atmospheres representing the stellar photosphere and, in addition, an expanding envelope of a specified density structure to account for the stellar wind. A recent review of results based on this model has been given e.g., by Wolf (1987). While these approaches can be justified for typical O-stars, it is obvious that in LBV's several assumptions inherent in these models are not valid. Most importantly, the continuum forming region of LBV's is clearly extended and the hydrodynamic and radiative properties of the wind and the photosphere may not be separated. Keeping in mind these considerations, we will not review previous attempts to model LBV's semi-theoretically but report on new methods now in progress.
     Our models make use of a spherically extended, dynamical NLTE atmosphere with 27 levels of H and He. The radiative transfer is calculated in the comoving frame. This code has been described in some detail by Hamann and Schmutz (1987). The effects of photospheric and wind blanketing due to metallic lines are accounted for empirically. We obtain the number of line scatterings relative to electron scatterings as a function of wind density from a Monte Carlo calculation following a photon on its way through the atmosphere. For a given pre-specified set of stellar parameters including the mass-loss rate

and the velocity law we obtain line profiles of H and He and the con-
tinuum energy distribution which are then compared with the observa-
tions.

The hydrodynamic structure of the wind is computed with a modi-
fied CAK code which does not make use of the radial streaming approx-
imation. The radiative acceleration is calculated from Abbott's
(1982) line list which is essentially complete up to Z = 30. The ion-
ization and excitation in the wind is treated as in Abbott and Lucy
(1985). Multi-line effects (multiple scatterings and line-overlap)
are empirically accounted for by a Monte Carlo simulation as described
above. The equation of motion of the flow is solved for a set of
stellar parameters which in turn leads to a prediction for the mass-
loss rate and the velocity field $v(r)$.

By combining the two codes for the radiative transfer and the
hydrodynamics we developed an iterative scheme to find a self-consis-
tent solution. The photospheric parameters, which are input for the
CAK code, are derived from the dynamical NLTE atmosphere as $R_{2/3}$ and
$T_{2/3}$, where 2/3 refers to the region in the atmosphere where Rosseland
optical depth 2/3 occurs. Using these photospheric parameters, we
obtain a hydrodynamic solution for the wind with a new mass-loss rate
and $v(r)$ which in turn leads to a new estimate for the multi-line
effects and can also be compared with the wind parameters derived from
the line-profile fitting.

The results presented here are based on a large number ($\sim$50) of
converged models obtained from the iteration scheme outlined above.

III. THE IONIZATION STATE OF THE ATMOSPHERE

A very striking property of LBV's from the point of view of a radia-
tively driven wind is the non-variable bolometric luminosity at dif-
ferent phases. Since a radiatively driven wind is primarily sensitive
to L, the huge $\dot{M}$ variations observed in LBV's between maximum and
minimum states are at first glance not obvious to understand in terms
of radiation pressure.

Figure 1 shows the observed energy distributions of R71 in its
minimum state and of R88 in its maximum state. Although the spectrum
of R71 shortward of $\sim$3000 Å has not been observed during its latest
maximum (around 1974), the close similarity in their stellar para-
meters implies that the IUE region of R71 at maximum should resemble
R88 at maximum. Notice the absence of the Balmer discontinuity in the
maximum as well as in the minimum phase emphasizing a very low gravity
and the importance of sphericity effects. The discontinuities visible
in the UV spectra are caused by line blanketing. The minimum spectrum
of R71 is blanketed by lines of (mostly) photospheric doubly ionized
iron-group elements. On the other hand, the spectrum of R88 at max-
imum shows very strong wind blanketing due to lines of singly ionized
iron-group elements. It is obvious that a self-consistent model of
the expanding atmospheres of R71 and R88 must account for these
dramatic changes in ionization and excitation.

Figure 2 shows the dependence of $\dot{M}$ and the terminal velocity v_∞
on the ionization state of the wind expressed by T_{ion}. The stellar
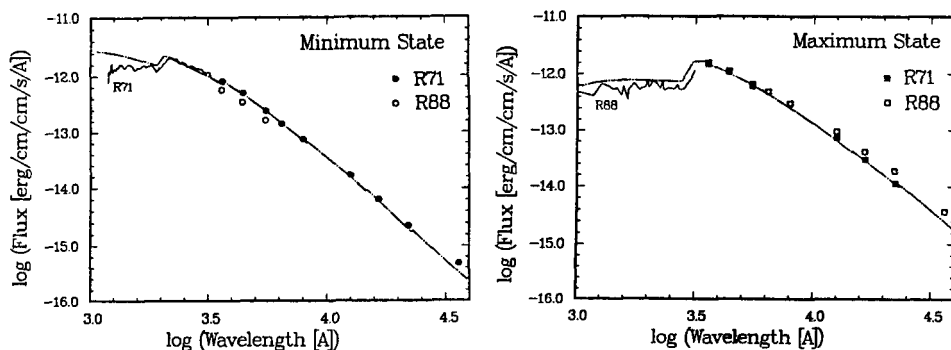
Fig. 1.   Observed and computed energy distributions of R71 and R88 at
          minimum and maximum states.

parameters refer to our final model of R71 in the minimum states (see
Table 1). In the right-hand section of the two figures the important
metallic lines driving the wind are doubly ionized, whereas on the
left side they are singly ionized. The strong sensitivity of $\dot{M}$ and
v_∞ can be explained by the different term schemes of singly and doubly
ionized iron-group elements. The important lines, which provide most
of the wind acceleration, are resonance lines, lines originating from
metastable levels, or other low-excitation lines, which are located
longward of 911 Å. (The stellar flux shortward of 911 Å is too small
for an efficient momentum transfer.) Doubly ionized iron-group
elements have most of their strong, low-lying transitions shortward of
911 Å, whereas longward of 911 Å most lines are due to transitions
with lower excitation potentials above ~5 eV. These lines can only be
excited collisionally. They are strong in the photosphere (cf. Figure
1) but not in the wind around the critical point. In contrast, singly
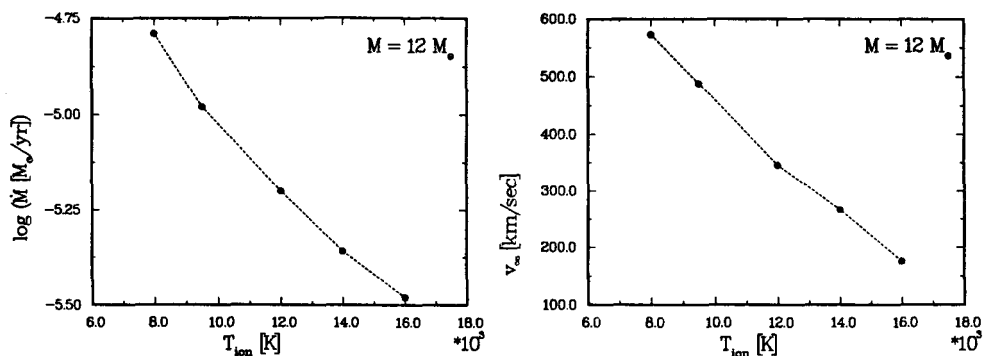ionized iron-group elements possess most of their strongest resonance

Fig. 2   Mass-loss rate and terminal velocity as a function of the
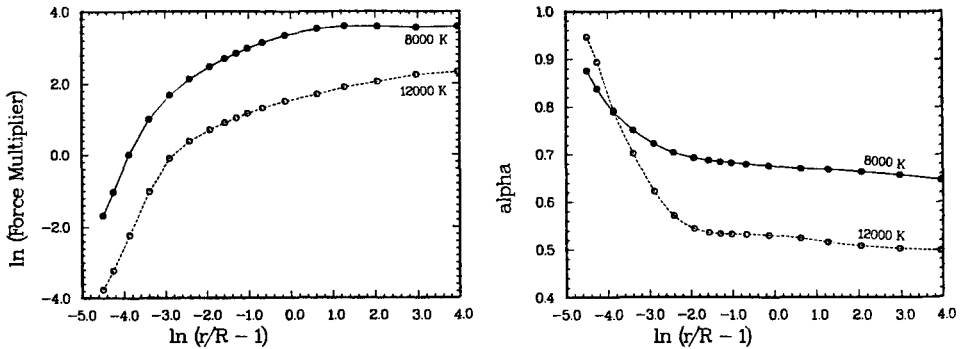   ionization state of the wind.

Fig. 3   Run of the force multiplier and α for two models with
          different values of T_{ion}.

lines longward of 911 Å in the Balmer continuum, which provides an
efficient momentum transfer from the stellar radiation field to the
stellar wind.

Figure 3 shows the behavior of the force multiplier (= the ratio
of acceleration due to lines and due to continuum) and α (= relative
fraction of optically thick [α=1] and thin [α=0] lines) in two repre-
sentative wind models. The model with T_{ion} = 8000 K has a higher line
acceleration and thus a higher mass-loss rate and a higher fraction of
optically thick lines producing a higher terminal velocity since
$v_\infty \sim \alpha/1-\alpha$ (cf. Kudritzki et al. 1987).

For reasons of clarity, the above discussion assumed identical
photospheric parameters for the maximum and minimum states, only T_{ion}
has been varied. This will now be relaxed, and we determine $R_{2/3}$ and
$T_{2/3}$ from an atmospheric fine analysis with our dynamical NLTE atmos-
phere. During all phases we have $R^2(2/3)\ T^4(2/3)$ = const. The
results derived above for Ṁ are virtually unaffected if one adopts the
photospheric parameters appropriate for a given T_{ion}. This is because
the stellar energy distribution in the Balmer continuum is not very
sensitive to a change in $T_{2/3}$ between 16000 K and 8000 K if L is
constant. On the other hand, log g is much lower in the maximum
state, and so is the surface escape velocity. Since the terminal
velocity of the wind scales with v_{esc}, we find that v_∞ is essentially
unchanged between the minimum and maximum states due to the counter-
acting influence of α and v_{esc}.

Table 1 presents the most important wind parameters of R71 in
maximum and minimum states derived from our hydrodynamic analysis.
The results are in good agreement with what is derived from a detailed
line profile and continuum analysis without making specific assump-
tions about the acceleration mechanism (see the poster by Leitherer et
al., these proceedings). This provides support for the assumption
that radiation pressure accelerates the stellar wind outside the opti-
cally thick photosphere.

Table 1. Converged hydrodynamic wind models for R71

	$T_{2/3}$	$R_{2/3}$	$\log \dot{M}$	v_∞	∞
Minimum	15500	88	-5.92	234	0.97
Maximum	8100	332	-4.79	259	1.1

IV. THE VARIATION OF THE PHOTOSPHERIC RADIUS

In our models the effective temperature and the stellar radius are
defined by

$$4\pi R_c^2 \, \sigma \, T_{eff}^4 = L$$

where the expansion velocity of the atmosphere is negligible at R_c.
Models which are very extended and/or have high mass-loss rates have
$T_{2/3} \neq T_{eff}$ and $R_{2/3} \neq R_c$. It appears attractive to interpret the
observed changes in $R_{2/3}$ and $T_{2/3}$ in terms of opacity effects, where
$R_{2/3}$ occurs further out in the atmosphere due to the higher wind den-
sities and R_c remains fixed. However, given the functional dependence
of $T(r)$, $v(r)$, and $\kappa\rho(r)$, we find that the difference between R_c and
$R_{2/3}$ is by far less than the observed factor-of-4 variation, even if
$\dot{M}$ is varied by a factor of 100. This conclusion is derived from our
line-profile and continuum analysis as well as from our hydrodynamic
calculations.
   Davidson (1987) discussed the relation between apparent tempera-
ture, the velocity of the photosphere, and $\dot{M}$ in LBV eruptions. Lamers
(1987) used this relation to derive a formula for the V-amplitude
between maximum and minimum states of an LBV and the difference in
$\dot{M}$. Our results disagree with this relation. While we agree with
Davidson's result that $T_{2/3}$ of R71 and R88 at outburst is around 8000
K, we disagree in that we can not simultaneously reproduce the
quiescent state of these stars with the same value of R_c; in other
words, these stars do not move along one of the graphs in Lamers'
(1987) Figure 2.
   Table 2 summarizes the photospheric parameters found for R71.
Notice the low gravity even in the minimum state and the low mass.
The IR energy distribution is severely affected by the low log g and
sphericity effects (as is the Balmer jump). The good agreement be-
tween observed and theoretical energy distribution (cf. Figure 1) is
due to the use of unified, extended model atmospheres. The "IR
excess" which arises when plane-parallel atmospheres without stellar
winds are compared to observations is accounted for self-consistently.

Table 2. Photospheric parameters of R71

	$\log L$	T_{eff}	R_c	$T_{2/3}$	$R_{2/3}$	$\log g$	M
Minimum	5.5	16000	84	15500	88	1.3	12
Maximum	5.5	10000	230	8100	332	0.0	12

114

We find a relatively extended subsonic region of v(r) with a very gradual acceleration and a steep velocity law in the wind region. This is in contrast to what is usually adopted for LBV's, namely a very shallow wind law (Leitherer et al. 1985, Waters and Wesselius 1986). Despite these differences, Ṁ derived here is not too different from what is published in the literature. This is due to the fact that a core-halo model with a linear v(r) happens to give the same answer when deriving Ṁ as does a unified, extended model with a hydrostatic density stratification plus a steep wind law.

V. CONCLUSIONS

Current spherical, dynamic models, which treat the radiation-hydro-dynamics in the expanding atmosphere self-consistently are in good agreement with the observations of R71 (and R88) at maximum and minimum states. The mass derived for R71 (~12 $M_\odot$) clearly hints at this LBV being a post-RSG. The same may be true for R88.
    Radiation pressure is able to account for the Ṁ variations between the minimum and maximum states due to the recombination of lines of doubly ionized iron-group elements in the relevant temper-ature regime. However, it is important to realize that this is no instability mechanism. Rather, it gradually operates between 16000 K and 8000 K. The drastic change in the photospheric radius observed in connection with the change of Ṁ can not be accounted for self-consis-tently in our models. Although recombination and ionization effects may be responsible for the so-called microvariability, which occurs in time-scales of weeks, it is hard to understand why these effects can account for variations on time-scales of decades. Probably the triggering mechanism has its origin in deeper, subphotospheric layers.

References
Abbott, D. C. 1982, Ap. J., **259**, 282.
Abbott, D. C., and Lucy, L. B., 1985, Ap. J., **288**, 679.
Davidson, K. 1987, Ap. J., **317**, 760.
Hamann, W.-R., and Schmutz, W. 1987, Astr. Ap., **174**, 173.
Kudritzki, R. P., Pauldrach, A., and Puls, J. 1987, Astr. Ap., **173**, 293.
Lamers, H. J. G. L. M. 1987, in Instabilities in Luminous Early-Type Stars, ed. H. Lamers and C. deLoore (Dordrecht: Reidel), p. 99.
Leitherer, C., Appenzeller, I., Klare, G., Lamers, H. J. G. L. M., Stahl, O., Waters, L. B. F. M., and Wolf, B. 1985, Astr. Ap., **153**, 168.
Waters, L. B. F. M., and Wesselius, P. R. 1986, Astr. Ap., **155**, 104.
Wolf, B. 1987, in IAU Symposium 122, Circumstellar Matter, ed. I. Appenzeller, C. Jordan (Dordrecht: Reidel), p. 409.

DISCUSSION

Appenzeller: Did I understand correctly that your minimum and maximum models result simply from using different core radii and that you can also produce (hypothetical) intermediate models by choosing an intermediate core radius?

Leitherer: Yes, we varied the core radius in the range implied by observations. We were not able to reproduce the observed energy distribution and line profiles with a fixed core radius and variable $R(\tau=2/3)$ only.

Cassinelli: Stellar interior theorists tell us that stars that lose mass and become quasi-homogeneous evolve to the left, toward the homogeneous-He-burning main sequence. Why does your star stop its leftward evolution around 16000 K?

Leitherer: Our models only try to reproduce the constraints given by the observations, *i.e.,* effective temperature between about 16000 K and 8000 K. The question of why the LBV phenomenon occurs just in this temperature region and what prevents the star from going leftward should be addressed to stellar-evolution theorists.

Langer: What relation is there between your proposed mass-loss-enhancing mechanism due to Fe recombination and the Munich group's model wherein LBV mass loss is provoked by the recombination of hydrogen?

Leitherer: Both mechanisms involve changes in the ionization conditions in the wind. The Fe II/III mechanism that I described in my talk, however, generates no instability or outburst. It operates relatively continuously in the relevant temperature region. We encountered instabilities several times in our series of model calculations with our core-halo CAK code, but they turned out to be artifacts when we tried to confirm them with our self-consistent Monte Carlo code.

Schmutz: It is important to realize that the mechanisms of S Dor type outbursts proposed by the Munich group (Pauldrach *et al.,* this meeting) and by us (Leitherer *et al.,* this meeting) are identical. The high mass-loss rate is due to Fe II lines, the low state occurs if iron is Fe III. Therefore it is only a question of the iron ionization balance in the wind whether the mass-loss rate is high or low. We achieved the ionization shift by adopting the observed temperatures of S Dor and R 71 in maximum and minimum states, respectively. The Munich group gets the ionization shift at constant temperature by increasing the mass-loss rate, *i.e.* by increasing the density in the wind.
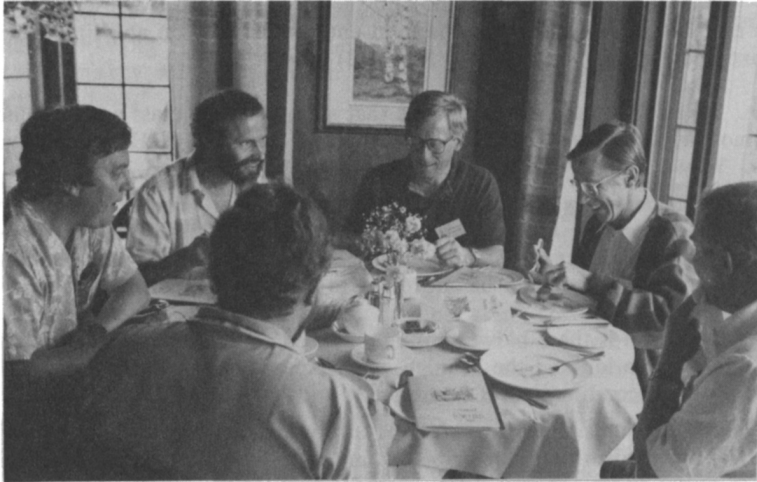
Williams, Balona, van der Hucht, Sterken